G.V. VERTSIMAKHA
Institute for Nuclear Research, Nat. Acad. of Sci. of Ukraine
(47, Prosp. Nauky, Kyiv 03680, Ukraine; e-mail: avertsim@kinr.kiev.ua)

PACS 73.20.Mf, 71.35.Cc, 87.14.E–

EFFECT OF THE RELATIVE SPATIAL ARRANGEMENT OF A METAL NANOSHELL AND AN LH2 COMPLEX OF PHOTOSYNTHETIC BACTERIA ON THE OPTICAL PROPERTIES OF THE HYBRID LIGHT-HARVESTING STRUCTURE

The influence of the relative spatial arrangement of a silver nanoshell and a peripheral LH2 complex of photosynthetic bacteria on the light absorption enhancement by the hybrid light-harvesting complex has been studied theoretically. The enhancement of light absorption in the interval of the B850 exciton band arises owing to the strong interaction between excitons in the LH2 ring and surface plasmons in the nanoshell. The range of hybrid structure parameters has been determined, at which the enhancement of the photosynthesis process efficiency in the presence of a silver nanoshell is possible.

Keywords: light-harvesting complex, nanoparticle, exciton, plasmon, photosynthetic bacterium.

1. Introduction

The unique optical properties of localized surface plasmons [1] invoke a wide interest of researchers owing to the opportunity of their application in biosensors [2], data storage devices [3], and surface-enhanced Raman spectroscopy [4]. The optical properties of various systems–in particular, the intensities of light absorption and luminescence by separate molecules, semiconductor quantum dots, and quantum wells–can substantially change in a vicinity of metal nanoparticles [5–9]. Experimental researches [10–15] and theoretical calculations [16, 17] also testify to the influence of nanoparticles on the efficiency of photosynthesis processes. In particular, the results of calculations obtained in work [17] demonstrate the growth of the probability of excited electron generation at the reaction center of photosystem I as a result of the interaction with plasmon excitations in gold or silver nanoparticles. In hybrid structures, which combine metallic and microbiological components, the properties of light-harvesting pigment-protein complexes can change as well. A growth in the fluorescence intensity of the light-harvesting complex of the marine alga *Amphidinium carterae* by an order of magnitude in a vicinity of silver nanoparticles was observed without a substantial variation of the radiation emission wavelength [10]. Metal nanoparticles can enhance the light absorption in photosystem I [18, 19]. The growth in the fluorescence intensity of separate light-harvesting LH2 complexes of photosynthetic purple bacteria was observed in a vicinity of the quasihexagonal lattice of spherical gold nanoparticles [16]. In the cited works, the matter concerned biological objects. Nevertheless, some optical processes in those structures can be explained in the framework of physical models that are well-known in the physics of molecular excitons [20], because the spectral properties of light-harvesting complexes of photosynthetic bacteria are governed by the exciton interaction between pigment molecules included into the given structures [21].

Metal nanoparticles can substantially affect the probability of exciton state excitation, provided the energy resonance between the nanoparticle plasmon state and the excitonic state of a molecular ring in the light-harvesting complex. This resonance can be obtained if a dielectric nanoparticle with a metal shell ("nanoshell") is used, because the resonance frequency of the surface plasmon state of the latter, in contrast to a continuous spherical metal nanoparticle, can be controlled by selecting the particle dimensions. In work [22], it was shown that, under definite conditions, the probability of light absorption and the energy transfer by the antenna light-harvesting complex can substantially increase in a vicinity of such silver metal nanoshells. However, the calculations in work [22] were carried out for a specific symmetric arrangement of a nanoparticle and the molecular ring of a light-harvesting LH2 complex with respect to each other. As a continuation of researches started in work [22], we consider in this work how the variation in the spatial position of nanoparticle with respect to the molecular ring of the antenna light-harvesting complex affects the efficiency of exciton-plasmon interaction and, as a consequence, the light absorption by this structure.

2. Model of the System: Excitons of the Antenna Light-Harvesting Complex, Plasmon States of a Metal Nanoparticle, and Their Interaction

The light absorption by photosynthetic pigments is one of the initial stages in the photosynthesis process. The so-called antenna (or light-harvesting) complexes of pigments absorb light and transmit the excitation to the reaction photosynthetic center, where the absorbed energy is spent in the course of photochemical reactions. Photosystems in the majority of purple bacteria contain light-harvesting complexes of two types: LH1 complexes, which are located near the reaction center, and peripheral LH2 complexes [23, 24]. Pigments of LH2 complexes, in comparison with those in LH1 ones, absorb light in the spectral interval with higher frequencies, which provides a consecutive energy transfer from LH2 to LH1 complexes and, ultimately, to the reaction center. The spatial structure and the exciton spectra of a light-harvesting LH2 complex in bacteria of various types were the object of numerous researches [24–33]. As is known, the bacteriochlorophyll (BChl) molecules in the light-harvesting LH2 complex of a photosynthesizing bacterium form two concentric rings characterized by the rotational symmetry C_9 (e.g., for bacteria *Rhodopseudomonas acidophila*) or C_8 (for bacteria *Rhodospirillum molischianum*). The internal ring is responsible for the absorption of light with a wavelength of 850 nm (the so-called B850 band) and contains 18 or 16 BChl molecules, which form the pairs of strongly coupled dimers with the distance between the neighbor pigments shorter than 1 nm [27]. This system can be simulated [21, 24, 28] as a molecular ring consisting of N molecules combined in pairs into $N/2$ equivalent dimers. As was shown in work [22], the presence of metal nanoparticles in a vicinity of this molecular ring in the light-harvesting complex can modify the optical properties of the latter; note that the calculations were carried out for a definite relative arrangement of the spherical nanoparticle and the ring, when the ring and nanoparticle centers lie on the axis directed perpendicular to the nanoring plane. A high symmetry degree of this system is responsible for certain regularities in the interaction between the exciton and plasmon states: one plasmon state can interact only with one definite exciton state (for other details, see work [22]). However, if the ring and the nanosphere are arranged arbitrarily with respect to each other, the symmetry of the system becomes broken (Fig. 1, *a*), which makes it impossible to find the wave function of the system analytically, as was done in work [22]. Hence, the issue of whether the light absorption enhancement by the light-harvesting complex still remains in this case should be additionally studied.

Consider the system consisting of a metal nanoparticle with dielectric core (a nanoshell) and a molecular ring located nearby (Fig. 1, *a*). The methods which will be used for the calculation of the exciton-plasmon interaction effects are similar to those proposed and described in work [22] in detail. Therefore, we confine the consideration to a short description of the basic theoretical propositions and the analysis of the results obtained. The Hamiltonian used for the description of this system was proposed in work [22]. It contains the following components: the Hamiltonian of a molecular ring, $\hat{H}_r$, the Hamiltonian of nanoparticles, $\hat{H}_p$, and a term $\hat{V}_{pr}$ describing the exciton-plasmon interaction,

$$\hat{H} = \hat{H}_r + \hat{H}_p + \hat{V}_{pr}. \quad (1)$$

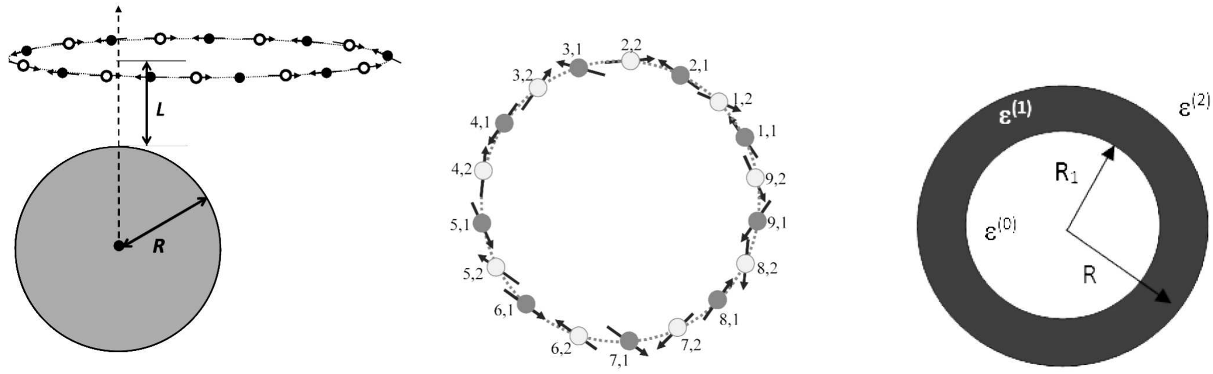

a *b* *c*

Fig. 1. Schematic diagram of the system consisting of a metal nanoparticle and the molecular ring B850 (*a*). Schematic diagram of the molecular ring B850 (*b*). Arrows designate the dipole moments of the molecules in the ring. Metal nanoshell with a dielectric core (*c*)

Below, each component of Hamiltonian (1) will be described in detail.

2.1. Molecular ring of a light-harvesting complex

When light is absorbed, a Frenkel exciton is excited in the molecular ring. It is described by the Hamiltonian [21]

$$\hat{H}_r = \sum_{n,\alpha} \hat{H}^0_{n\alpha} + \sum_{n\alpha,n'\alpha'} V_{n\alpha,n'\alpha'} \hat{B}^+_{n\alpha} \hat{B}_{n'\alpha'}, \tag{2}$$

where $\hat{H}^0_{n\alpha} = E_\alpha \hat{B}^+_{n\alpha} \hat{B}_{n'\alpha'}$ is the Hamiltonian of the molecule; $\hat{B}^+_{n\alpha}$ and $\hat{B}_{n\alpha}$ are the creation and annihilation, respectively, operators of electron excitation of the molecule with the number $n\alpha$; n is the dimer number; $\alpha = 1, 2$ is the number of the molecule in the dimer; E_α is the excitation energy; and $V_{n\alpha,n'\alpha'}$ is the matrix element of the interaction between the molecules $n\alpha$ and $n'\alpha'$. The molecules in the ring that form a dimer differ by the orientation of their dipole moments of excitonic transition (Fig. 1, *b*). The presence of two molecules in an elementary cell of the ring gives rise to the Davydov splitting of the excitonic band into two ones, which we will mark by the index $i = +$ or $-$; namely [25],

$$E_\pm = \frac{1}{2}\Big[E_1 + E_2 + V_{11} + V_{22} \pm$$

$$\pm\sqrt{(E_1 - E_2 + V_{11} - V_{22})^2 + 4V_{12}V_{21}}\Big], \tag{3}$$

where $V_{\alpha\beta}(k) = \sum_{n'} V_{n\alpha,n'\beta} e^{ik(n-n')}$; the quantity $k = 2\pi l_k/N$ determines the quantum number of an excitonic state of the ring; and $l_k = 0, \pm1, \pm2, ...,$ $\pm\,[N/4]$ if $N/2$ is odd or $l_k = 0, \pm1, \pm2, ..., \pm[N/4]-1,$ $[N/4]$ if $N/2$ is even, where the brackets mean the integer part of the corresponding number. Below, the exciton states of the molecular ring will be enumerated with the use of the variables l_k and i. The excitonic spectra of the molecular ring were calculated in the framework of the dipole-dipole approximation, with the value taken for the matrix element of the dipole moment of the excitonic transition being typical of a bacteriochlorophyll molecule [34]. The other parameters were selected as follows: $E_1 = 12\,500$ cm^{-1}, $E_2 = 12\,800$ cm^{-1}, and the radius of molecular ring was equal to 2.7 nm [34]. The obtained spectrum of the molecular ring with $N = 18$ is depicted in Fig. 2. The excitonic levels of the ring are twice degenerate, except for the states with $l_k = 0$ and (for even values of $N/2$) $l_k = [N/4]$. In the dipole approximation, only the states with $l_k = \pm1$ participate in the absorption of a photon with the polarization vector parallel to the ring plane, and the oscillator strength for the states with $i = +$ is much weaker than that with $i = -$. The excitation of the states with $l_k = 0$ is also allowed for photons polarized normally to the ring plane. However, the oscillator strength of such transitions is very weak.

2.2. Nanoparticle with a metal shell

Dielectric particles with metal shells (nanoshells) are a promising object for the researches of surface plasmon excitations in nanoobjects [35]. Modern technologies allow similar particles to be grown up with various dimensions and shapes, as well as various metals to be used for the creation of an external shell. Silicon, a material with an extremely low dielectric constant [36], is often used as a core material for such particles. Hollow metallic nanoshells are also grown up nowadays [37]. An advantage of nanoparticles with a metallic shell over all-metal nanoparticles in the plasmon studies consists in the possibility to affect the frequency of plasmon oscillations by varying the thickness of the metallic layer. This fact is especially important while studying the interaction of plasmons with another subsystem, in particular, as occurs in the problem concerned, with the molecular ring, because it is necessary to obtain a resonance between the energy levels of subsystems. The frequencies of plasmon oscillations in a particle with the dielectric core radius R_1, the external radius R, and the dielectric constants of the core, $\varepsilon^{(0)}$, the metallic shell, $\varepsilon^{(1)} = \varepsilon_{m0} - \omega_p^2/\omega^2$, and the environment, $\varepsilon^{(2)}$, (see Fig. 1,*b*) are the solution of the electrodynamic problem in the quasistatic approximation [22],

$$\left(\frac{\omega_l^{\pm}}{\omega_p}\right)^2 = -\frac{A_l^{11} + A_l^{22}}{2} \pm \sqrt{\frac{\left(A_l^{11} - A_l^{22}\right)^2}{4} + A_l^{12} A_l^{21}}, \tag{4}$$

where

$$A_l^{11} = -\frac{l}{\Delta_l}\left\{\frac{\left(\varepsilon^{(2)} - \varepsilon_{m0}\right)(l+1)}{R^{2l+1}} + \right.$$

$$\left. + \frac{\varepsilon^{(0)} l - \varepsilon_{m0}(l+1)}{R_1^{2l+1}}\right\},$$

$$A_l^{12} = \frac{l+1}{R^{2l+1} R_1^{2l+1} \Delta_l}\left(\varepsilon^{(2)}(l+1) + \varepsilon^{(0)} l\right),$$

$$A_l^{21} = \frac{l}{\Delta_l}\left(\varepsilon^{(2)}(l+1) + \varepsilon^{(0)} l\right),$$

$$A_l^{22} = \frac{l+1}{\Delta_l}\left\{\frac{l\left(\varepsilon_{m0} - \varepsilon^{(0)}\right)}{R^{2l+1}} - \frac{\varepsilon^{(2)}(l+1) + l\varepsilon_{m0}}{R_1^{2l+1}}\right\},$$

$$\Delta_l = \frac{l(l+1)}{R^{2l+1}}\left(\varepsilon^{(2)} - \varepsilon_{m0}\right)\left(\varepsilon_{m0} - \varepsilon^{(0)}\right).$$

For silver, the plasmon frequency $\hbar\omega_p = 11.5853$ eV and $\varepsilon_{m0} = 8.926$ [38]. The appearance of two characteristic frequencies for the given quantum numbers l and m is connected with the presence of two metal surfaces of the particle [39]. Therefore, the frequencies are enumerated with the help of the indices l, m, and j, where j denotes the solution branch, $j = \pm$. Hence, plasmon excitations of the nanoparticle are described by the Hamiltonian

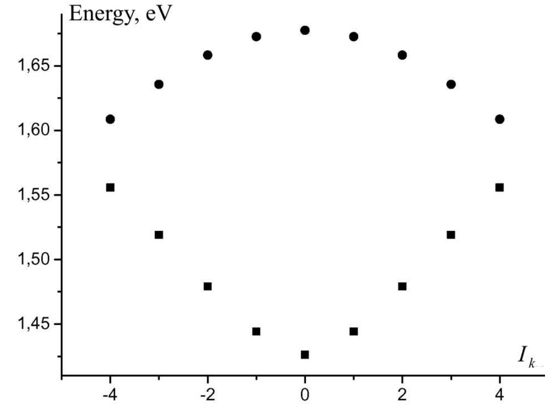

Fig. 2. Exciton spectrum of a molecular ring with $N = 18$. Circles and squares denote states with $i = +$ and $i = -$, respectively

$$H_p = \sum_{lmj} \hbar\omega_l^j \hat{A}_{lmj}^{+} \hat{A}_{lmj}, \tag{5}$$

where $\hat{A}_{lmj}^{+}$ and $\hat{A}_{lmj}$ are the creation and annihilation, respectively, operators of a surface plasmon in the state with the orbital and magnetic quantum numbers l, m, and j, respectively. In what follows, only the interaction of exciton states with the lower-energy plasmon branch ($j = -$) will be taken into account.

2.3. Exciton-plasmon interaction

In work [22], we derived an expression for the operator of electric potential created at a certain point $\mathbf{r} = (r, \theta, \phi)$ in space by the surface plasmon excitations in a metallic nanoshell,

$$\hat{\phi}(\mathbf{r}) = \sum_{l,m,j=\pm}\left(\hat{A}_{lmj}\tilde{\phi}_{lmj}(\mathbf{r}) + \hat{A}_{lmj}^{+}\tilde{\phi}_{lmj}^{*}(\mathbf{r})\right), \tag{6}$$

where

$$\tilde{\phi}_{lmj}(\mathbf{r}) = \frac{K_l^j}{2}\sqrt{\frac{\hbar}{4\omega_l^j b_l^j}}\frac{Y_{lm}(\theta,\, \phi)}{r^{l+1}},$$

$$K_l^j = \left(A_l^{11} R^{2l+1} + A_l^{21} - \right.$$

$$\left. - \frac{\left(\omega_l^j\right)^2 + \omega_p^2 A_{lm}^{11}}{\omega_p^2 A_l^{11}}\left(A_l^{12} R^{2l+1} + A_l^{22}\right)\right),$$

$$b_l^j = \frac{\left(R^{2l+1} - R_1^{2l+1}\right)}{8\pi\omega_p^2}\left[l + \frac{l+1}{R^{2l+1}R_1^{2l+1}}\times\right.$$
$$\left.\times\left(\frac{\left(\omega_l^j\right)^2 + \omega_p^2 A_l^{11}}{\omega_p^2 A_l^{11}}\right)^2\right].$$

The exciton-plasmon interaction is affected by the electric field created by a surface plasmon on the dipole moments of ring's molecules,

$$\hat{V}_{pr} = \sum_{n\alpha} \hat{\mathbf{p}}_{n\alpha} \nabla \hat{\varphi}_{lmj}^{n\alpha}, \tag{7}$$

where $\hat{\varphi}_{lmj}^{n\alpha}$ is the operator of the electric potential (6) that acts on the molecule with the number (n, α), and $\hat{\mathbf{p}}_{n\alpha}$ is the dipole moment operator for the given molecule. Seeking the solution of the Schrödinger equation with Hamiltonian (1) in the form of a superposition of the nanoparticle plasmon states and the exciton states of the molecular ring,

$$\Psi = \sum_{k,i} \alpha_{ki} \hat{B}_{ki}^{+} \left|0\right\rangle + \sum_{l,m,j} \beta_{lmj} \hat{A}_{lmj}^{+} \left|0\right\rangle, \tag{8}$$

we obtain the following system of equations for the coefficients α_{ki} and β_{lmj}:

$$\alpha_{ki}\left(E_{ki} - E\right) + \sum_{n,\alpha,l,m,j} \mathbf{d}_{n\alpha}^{*} \nabla \tilde{\phi}_{lmj}^{n\alpha} a_{n\alpha}^{ki} \beta_{lmj} = 0, \tag{9}$$

$$\beta_{lmj}\left(\hbar\omega_{lj} - E\right) + \sum_{k,i,n,\alpha} \mathbf{d}_{n\alpha} \nabla \tilde{\phi}_{lmj}^{n\alpha *} a_{n\alpha}^{ki*} \alpha_{ki} = 0, \tag{10}$$

It was shown in work [22] that, in the case of a symmetric subsystem configuration where the centers of the nanosphere and the ring lie on the axis directed perpendicularly to the ring plane and in the dipole approximation, the interaction results in that only definite states of the subsystems become mixed. Indeed, owing to the symmetry of the problem, the majority of interaction matrix elements in Eqs. (9) and 10) equal zero. In this case, the corrections to the energies of quantum states and the coefficients can be calculated analytically. However, if the nanoparticle is located arbitrarily with respect to the ring, the problem must be solved numerically with regard for all terms in the system. The corresponding results are presented below.

The determining characteristic of the optical properties of the system hybrid states is the matrix element of the operator describing the total dipole moment of the system,

$$\hat{\mathbf{P}} = \hat{\mathbf{P}}_r + \hat{\mathbf{P}}_p, \tag{11}$$

where $\hat{\mathbf{P}}_r = \sum_{n,\alpha}\left(\mathbf{p}_{n\alpha}\hat{B}_{n\alpha}^{+} + \mathbf{p}_{n\alpha}^{*}\hat{B}_{n\alpha}\right)$ is the operator of the ring dipole moment, which is a sum of the dipole moments of all molecules; and $\hat{\mathbf{P}}_p$ is the operator of the nanoparticle dipole moment, the expression for which can be obtained from the dipole term in the series expansion of the nanoparticle potential operator (6). Using the wave function (8), we can obtain an expression for the squared absolute value of the matrix element for the dipole transition of the system from the ground state into an excited one ν, $\left|\mathbf{P}_{0\to\nu}\right|^2$, which characterizes the probability of light absorption at the excitation of this state. The exciton-plasmon interaction brings about a redistribution of the transition dipole moment between the nanoparticle plasmon states and the ring exciton states. Since the multielectron plasmon states of a nanoshell are characterized by a large dipole moment, an admixture of even an insignificant fraction of the plasmon state results in a strong growth of the dipole moment of hybrid states. The effect becomes stronger, when the energies of the exciton and plasmon states come closer to each other. This can be reached by changing the thickness of nanoparticle's metallic layer. While calculating the matrix element of the transition dipole moment, the damping of surface plasmon states was made allowance for by introducing the imaginary part of the plasmon energy, $\hbar\omega_l^j \to \hbar\omega_l^j - i\hbar\Gamma$. This radiationless absorption is associated with the interaction between the plasmon state and the other states in the electron spectrum of a metal; it affects the exciton states of the ring owing to the hybridization of states. The widths of the plasmon bands, which are related to this damping, considerably exceed the bandwidths of exciton states in the ring; therefore, the latter are neglected. This means that the lifetime of a hybrid state of the system in the adopted model is governed exclusively by the lifetime of plasmon states.

3. Results and Their Discussion

Figure 3 demonstrates how the energies of some lowest states in the hybrid system are changed, when the ring is shifted with respect to the nanoparticle. In the figure, the zero shift, $x = 0$, corresponds to the maximally symmetric position of the ring with respect to the nanoparticle, when the centers of the ring and the nanosphere lie on the axis directed perpendicularly to the ring plane. Not going beyond the limits of this plane (the membrane plane), let us shift the ring in a certain direction, which is selected as the axis OX. A different shift direction does not change the results of calculations qualitatively and changes them quantitatively very weakly, because the ring is rather symmetric with respect to its rotations in this plane. The interaction with the nanoparticle weakly changes the energy levels in the ring. At $x = 0$ (this is a configuration, which was considered in work [22]), only the exciton levels with $l_k = \pm 1$ and plasmon ones with $m = \pm 1$ are shifted; because, as was mentioned above, the other exciton states do not interact with the dipole plasmon states owing to the problem symmetry. When the ring is shifted from this symmetric position by a distance of the order of the nanoparticle radius, the other exciton states of the ring start to interact with plasmons as well; in addition, the degeneration of states becomes eliminated.

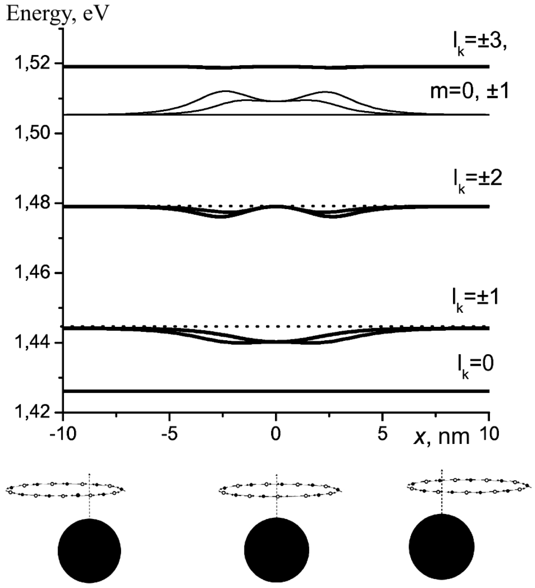

Fig. 3. Energies of some lowest states in the system as functions of the ring shift with respect to the center of a metal nanoparticle of the radius $R = 3$ nm for the parameters $\varepsilon^{(0)} = 1.4$, $\varepsilon^{(2)} = 1$, $\hbar\Gamma = 0.1$ eV, $L = 0$, and the internal radius $R = 2.9$ nm. Bold curves correspond to exciton states, thin curves to plasmon states, branches $j, i = -$. Dotted lines exhibit the levels of an isolated molecular ring

To make a quantitative evaluation of the optical absorption enhancement by the exciton subsystem, we calculated the ratios between the squared absolute values of the dipole moment matrix elements for transitions into every possible states of the system and the corresponding value for the lowest excitonic transition in the molecular ring in the absence of a nanoparticle, $\delta_\nu = |\mathbf{P}_{0\rightarrow\nu}|^2/|\mathbf{P}_r^0|^2$. In Fig. 4, the results of calculations for the dependence of δ_ν on the shift x from the symmetric position of the ring with respect to the silver nanoparticle 3 nm in radius with the internal radius of the dielectric core equal to 2.9 nm are shown for some system states. The bold solid and dashed curves correspond to the exciton states with $l_k = \pm 1$ and $i = -$, which can be excited both in the absence of a nanoparticle ($x \to \infty$) and when the latter is arranged symmetrically ($x = 0$). The transitions into other exciton states of the system (their δ_ν-dependences are plotted by thin solid curves) are forbidden at $x = 0$ owing to system's symmetry. The shift of a nanoparticle with respect to the ring breaks system's symmetry, and those transitions become allowed. An enhancement of those additional transitions can be seen especially pronounced, when the ring is located close up to the nanoparticle surface (Fig. 4,*a*). However, this arrangement cannot be realized in a real light-harvesting system, because the thickness (from 3.6 [40] to 5 nm [41]) of the membrane containing the molecular ring has to be taken into consideration. Figure 4,*b* demonstrates the results of calculations in the geometry where the distance between the ring plane and the nanoparticle surface equals 1.5 nm. If the nanoparticle is shifted, the light absorption enhancement takes place for the majority of system's states. Analogously to the case of a symmetric configuration of the system considered in work [22], this phenomenon is more pronounced for large nanoparticles (Fig. 5). In contrast to particles with small radii, the dipole moments of all transitions, except for the transitions into states with $l_k = \pm 1$, remain small for nanoparticles 20–30 nm in radius, when the ring is shifted. This follows from the fact that, in the case where the nanoparticle radius exceeds that of the molecular ring by an order of magnitude, the electric field cre-

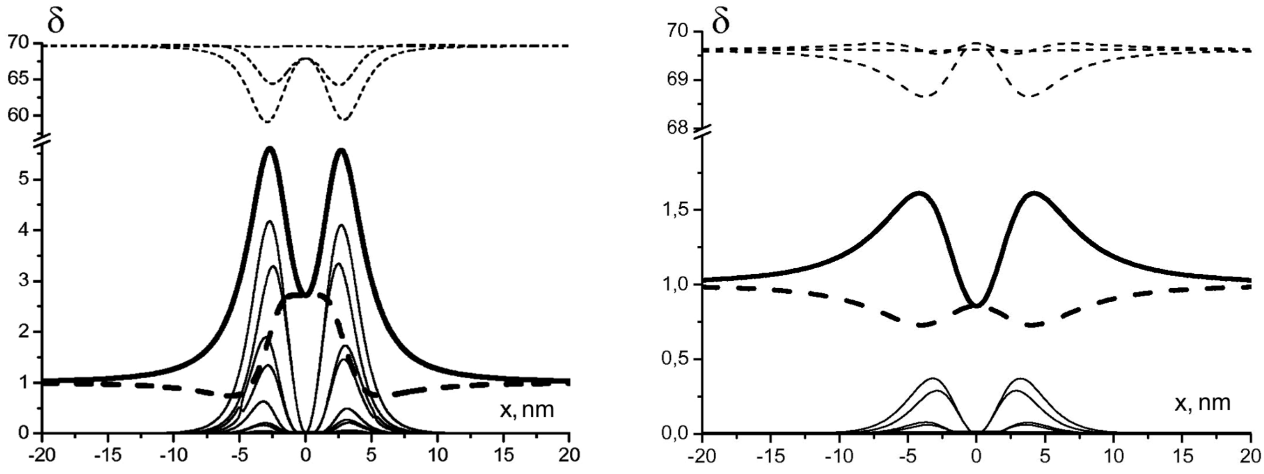

a *b*

Fig. 4. Optical absorption enhancement as a function of the ring shift with respect to the center of a metal nanoparticle with small radius. Bold solid and dashed curves correspond to the states with $l_k = \pm 1$ and $i = -$, thin solid curves to transitions into other exciton states of the system, thin dashed lines to plasmon states. The external nanoshell radius $R = 3$ nm, the internal radius $R_1 = 2.9$ nm, $\varepsilon^{(0)} = 1.4$, $\varepsilon^{(2)} = 1$, and $\hbar\Gamma = 0.1$ eV. (*a*) The ring is located close up to the nanoparticle ($L = 0$); (*b*) the distance between the nanoparticle surface and the ring plane $L = 1.5$ nm

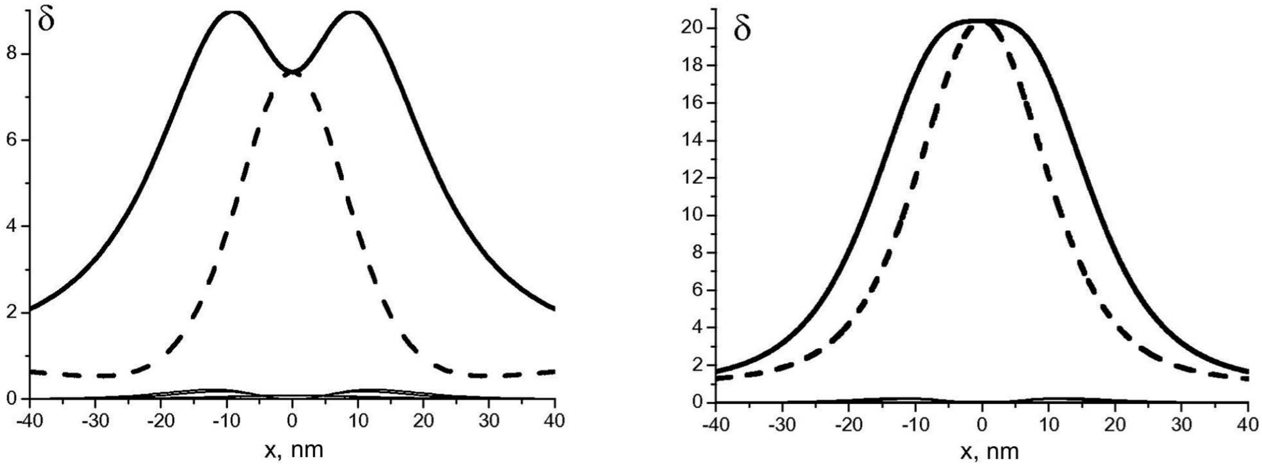

a *b*

Fig. 5. Optical absorption enhancement as a function of the ring shift with respect to the center of a metal nanoparticle with large radius. Bold solid and dashed curves correspond to the states with $l_k = \pm 1$ and $i = -$; excitation of other exciton states of the system (thin solid curves) are much less probable; curves corresponding to plasmon states are not shown. The external nanoshell radius $R = 20$ nm, $\varepsilon^{(0)} = 1.4$, $\varepsilon^{(2)} = 1$, $\hbar\Gamma = 0.1$ eV, the distance between the nanoparticle surface and the ring plane $L = 1.5$ nm, the internal radius $R_1 = 19.3$ (*a*) and 19.4 nm (*b*)

ated by plasmon excitations practically is not changed at distances equal to intermolecular distances in the ring, so that the symmetry of the arrangement of dipole molecular moments in the ring becomes an important factor. In this case, Eqs. (9) and (10) will contain sums of the form $\sum_n \mathbf{p}^*_{n\alpha} \exp\left(i\frac{2\pi l_k n}{N}\right)$, which differ from zero for the given ring-like structure only if $l_k = \pm 1$. The calculations testify that the effect of absorption enhancement for the states with $l_k = \pm 1$ remains substantial if the ring is shifted from its symmetric position by a distance close to the nanoparticle radius. The average distance between the centers of LH2 complexes of bacteria *Rhodobacter sphaeroides* amounts to 8.5 nm [42], which corresponds to a surface complex density of 10^{12} cm^{-2}. In the case of relatively large nanoparticles (their data are shown in Fig. 5), the enhancement effect will be appreciable, provided that the molecular ring is located at a distance of 25-30 nm from the particle center, i.e. a single nanoparticle will enhance the absorption of about 30 light-harvesting LH2 complexes.

4. Conclusions

This work continues our researches [22] concerning the interaction between a light-harvesting LH2 complex of photosynthesizing bacteria and a silver nanoshell, in which the hybridization of exciton and plasmon states is shown to result in the enhancement of light absorption by the hybrid system. We have shown that the optical absorption enhancement, which is associated with the transfer of the intensity from the plasmon dipole transition to the excitonic one, survives if the symmetry of a spatial arrangement of the nanoshell with respect to the molecular ring of a light-harvesting complex is violated. For nanoparticles with small radii (of about the ring radius) located asymmetrically with respect to the molecular ring, the absorption is additionally enhanced due to the appearance of transitions that are forbidden in the case of a symmetric arrangement. For the nanoshells of large (in comparison with the ring radius in the light-harvesting complex) radii, the light absorption enhancement remains substantial if the spherical nanoparticle is shifted in the membrane plane by a distance close to the nanoshell radius.

The author expresses her gratitude to Profs. V.I. Sugakov and I.Yu. Goliney for the formulation of the problem and the useful discussion.

1. A.V. Zayats, I.I. Smolyaninov, and A.A. Maradudin, Phys. Rep. **408**, 131 (2005).
2. K. Aslan, J.R. Lakowicz, and C.D. Geddes, Curr. Opin. Chem. Biol. **9**, 538 (2005).
3. J. Tominaga, C. Mihalcea, D. Buechel *et al.*, Appl. Phys. Lett. **78**, 2417 (2001).
4. K. Kneipp, Y. Wang, H. Kneipp *et al.*, Phys. Rev. Lett. **78**, 1667 (1997).
5. W. Zhang, A.O. Govorov, and G.W. Bryant, Phys. Rev. Lett. **97**, 146804 (2006).
6. S.M. Sadeghi, Phys. Rev. B **79**, 233309 (2009).
7. V.I. Sugakov and G.V. Vertsimakha, Phys. Rev. B **81**, 235308 (2010).
8. P. Anger, P. Bharadwaj, and L. Novotny, Phys. Rev. Lett. **96**, 113002 (2006).
9. S. Kuhn, U. Hakanson, L. Rogobete, and V. Sandoghdar, Phys. Rev. Lett. **97**, 017402 (2006).
10. V. Nagarajan and W.W. Parson, Biochemistry **36**, 2300 (1997).
11. L. Bujak, D. Piatkowski, S. Mackowski *et al.*, Acta Phys. Pol. A **116**, S22 (2009).
12. L. Bujak, B. Krajnik, M. Olejnik *et al.*, Photonics Lett. Pol. **4**, 14 (2012).
13. L.Du, Y.Huang, B.Ren, and Y.Weng, J. Phys. Chem. C **116**, 6993 (2012).
14. I. Carmeli, I. Lieberman, L. Kraversky *et al.*, Nano Lett. **10**, 2069 (2011).
15. N. Czechowski, P. Nyga, M.K. Schmidt *et al.*, Plasmonics **7**, 115 (2012).
16. S.R. Beyer, S. Ullrich, S. Kudera *et al.*, Nano Lett. **11**, 4897 (2011).
17. A. Govorov and I. Carmeli, Nano Lett. **7**, 620 (2007).
18. I. Kim, S.L. Bender, J. Hranisavljevic *et al.*, Nano Lett. **11**, 3091 (2011).
19. S. Mackowski, J. Phys. Condens. Matter **22**, 193118 (2010).
20. A.S. Davydov, *Theory of Molecular Excitons* (Plenum Press, New York, 1971).
21. X. Hu and X. Schulten, Phys. Today **50**, No. 8, 28 (1997).
22. I.Yu. Goliney, V.I. Sugakov, L. Valkunas, and G.V. Vertsimakha, Chem. Phys. **404**, 116 (2012).
23. R. Van Grondelle and V. I. Novoderezhkin, Nature **463**, 614 (2010).
24. M.Z. Papiz, S.M. Prince, A.M. Hawthornthwaite-Lawless *et al.*, Science **1**, 198 (1996).
25. R.E. Blankenship, *Molecular Mechanisms of Photosynthesis* (Wiley-Blackwell, Malden, MA, 2002).
26. G. McDermott, S.M. Prince, A.A. Freer *et al.*, Nature **374**, 517 (1995).
27. J. Koepke, X. Hu, C. Muenke *et al.*, Structure **4**, 581 (1996).
28. V. Novoderezhkin and A. Razjivint, Biophys. J. **68**, 1089 (1995).
29. V. Urboniene, O. Vrublevskaja, A. Gall *et al.*, Photosyn. Res. **86**, 49 (2005).
30. V. Urboniene, O. Vrublevskaja, G. Trinkunas *et al.*, Biophys. J. **93**, 2188 (2007).
31. M.V. Mostovoy and J.Knoerster, J. Phys.Chem. B **104**, 104 (2000).
32. R.J. Gordell and J. Konler, Biochem. J. **422**, 193 (2009).
33. J. Strumpfer and K. Schultena, J. Chem. Phys. **131**, 225101 (2009).

34. M.H.C. Koolhaas, G. van der Zwan, and R. van Grondelle, J. Phys. Chem. B **104**, 4489 (2000).
35. S. Kalele, S.W. Gosavi, J. Urban, and S.K. Kulkarni, Curr. Sci. **91**, 1038 (2006).
36. D. Shamiryan, T. Abell, F. Iacopia *et al.*, Mat. Today **7**, 34 (2004).
37. X.W.D. Lou, L.A. Archer, and Z. Yang, Adv. Mater. **20**, 3987 (2008).
38. M. Sukharev, J. Sung, K.G. Spears *et al.*, Phys. Rev. B **76**, 184302 (2007).
39. E. Prodan and P. Norlander, Nano Lett. **3**, 543 (2003).
40. K.-H. Rhee, Annu. Rev. Biophys. Biomol. Struct. **30**, 307 (2001).
41. E.H. Pape, W. Menke, D. Weick *et al.*, Biophys. J. **30**, 221 (1974).
42. J.D. Olsen, J.D. Tucker, J.A. Timney *et al.*, J. Biol. Chem. **283**, 30772 (2008).

Received 27.02.13.
Translated from Ukrainian by O.I. Voitenko

Г.В. Верцімаха

ВПЛИВ ВЗАЄМНОГО ПРОСТОРОВОГО ПОЛОЖЕННЯ МЕТАЛЕВОЇ НАНОЧАСТИНКИ ТА LH2 КОМПЛЕКСУ ФОТОСИНТЕТИЧНИХ БАКТЕРІЙ НА ОПТИЧНІ ВЛАСТИВОСТІ ГІБРИДНОЇ СВІТЛОЗБИРАЛЬНОЇ СТРУКТУРИ

Резюме

Теоретично досліджено залежність ефекту підсилення поглинання світла від взаємного розташування срібної нанооболонки та периферичного LH2 комплексу фотосинтетичних бактерій в гібридній світлозбиральній структурі. Ефект підсилення поглинання світла у смузі B850 зумовлений сильною взаємодією екситонів LH2-кільця та поверхневих плазмонів нанооболонки. Визначено діапазон параметрів гібридної структури, для яких присутність срібної нанооболонки веде до підвищення ефективності процесів фотосинтезу.